United States Department of Agriculture

NRCS

Natural Resources Conservation Service
National Soil Survey Center
Federal Building, Room 152
100 Centennial Mall North
Lincoln, NE 68508-3866

Phone: (402) 437-5499
FAX: (402) 437-5336

SUBJECT: SOI – Geophysical Assistance

November 22, 2011

TO: Travis Neely
State Soil Scientist/MLRA Office Leader
USDA-Natural Resources Conservation Service
6013 Lakeside Boulevard
Indianapolis, IN 46278

File Code: 330-7

Dr Philip Owens
Assistant Professor of Agronomy
Department of Agronomy, 915 West State Street
West Lafayette, IN 47907-2054

Purpose:
The purpose of this investigation is to use geophysical methods to conduct a soil-landscape study of a small catchment located at the Southern Indiana-Purdue Agricultural Center near Dubois, Indiana. The objective of this research is to develop improved models of the distribution of soils and soil properties as related to differences in parent materials and landforms, and to better understand the movement of water across soil-landscape components.

Participants:
Jim Doolittle, Research Soil Scientist, USDA-NRCS-NSSC, Newtown Square, PA
Richard Jones, Soil Scientist, USDA-NRCS, Huntington, WV
Dr Philip Owens, Assistant Professor of Agronomy, Purdue University, Lafayette, IN

Activities:
Field activities were completed during the period of 16 to 19 May 2011.

Summary:

1. Electromagnetic induction (EMI) data were collected across the catchment. This data can be used to improve the soil map, evaluate soil-landscape relationships, and assess temporal and spatial variations in soil moisture and preferential movement of water across different soil-landscape components. The present survey was conducted in the spring, when soil moisture is at a high level. To assess temporal variations in soil moisture, this catchment should be return to in the fall, when soil moisture contents are at lower levels, and the EMI survey repeated. Differences in apparent conductivity (EC_a) between the two surveys can then be used to infer temporal differences in the distribution of soil moisture.

2. Using EMI, the catchment was quickly surveyed and, with the aid of ground-truth auger observations, spatial patterns of EC_a were associated with different soil-landscape components. Mapped as Wellston soils (WeC2), higher-lying summit and upper side slopes components have conspicuously higher EC_a. Ground-truth auger observations revealed a close

similarity of the soils on these landscape components to the Tilsit series. Tilsit soils can formed in a loess mantle overlying a fine-textured residuum, weathered from sandstone, siltstone, and shale. Higher EC_a in areas of Tilsit soils is principally associated with the higher clay content of the residuum. Lower side slopes and foot slopes have lower conductivity and correspond to areas of Gilpin soils, which are moderately deep to fractured bedrock. The lower EC_a in areas of Gilpin soils is principally associated with lower clay contents and shallower depths to electrically resistive bedrock.

3. Within the catchment, GPR was effectively used to identify soils based on soil depth criteria, profile the bedrock topography, and characterize soil, lithologic and stratigraphic layers. The use of two geophysical tools provided complementary information, which provides greater confidence in interpretations.

4. A file of the EMI data has been sent by e-mail to Dr Owens.

It was the pleasure of Jim Doolittle and the National Soil Survey Center to be of assistance to you and Dr Owens in this study.

/s/ Jonathan W. Hempel

JONATHAN W. HEMPEL

Director

National Soil Survey Center

cc: See attached list

cc:

Jim Doolittle, Research Soil Scientist, NSSC, USDA-NRCS, 11 Campus Blvd., Suite 200, Newtown Square, PA 19073
Michael Golden, Director of Soils Survey Division, USDA-NRCS, Washington, DC 20250
Richard Jones, Soil Scientist, USDA-NRCS, 2631 5th Street Road, Huntington, WV 25701
Dave Kingsbury, MLRA Office Leader, USDA-NRCS, 1550 Earl Core Road, Suite 200, Morgantown, WV 26505
Wes Tuttle, Soil Scientist (Geophysical), USDA-NRCS-NSSC, P.O. Box 60, 207 West Main Street, Rm. G-08, Federal Building, Wilkesboro, NC 28697
Larry West, National Leader for Soil Survey Research and Laboratory Staff, USDA-NRCS-NSSC, Lincoln, NE
Douglas A. Wysocki, Research Soil Scientist & Liaison for MO10, Soil Survey Research and Laboratory Staff, USDA-NRCS-NSSC, Lincoln, NE

Technical Report On The Use Of Geophysical Methods For The Evaluation Of Soil Structures And Hydrologic Processes Within A Small Catchment Located In Dubois County, Indiana, 16 To 19 May 2011.

James A. Doolittle

Background:
With increased access to GIS, digital elevation models, remote sensing, and geophysical data sets, there are increasing trends towards more quantitative assessments of soils and hydrologic properties (Bui, 2004). Quantifying soil properties and hydrologic processes at different spatio-temporal scales remains a major challenge in hydropedology. Soil-water interactions and landscape-soil-hydrology relationships at different spatial scales (e.g., pedon, watershed, and regional) are exceedingly complex and variable. Soil properties (e.g., horizonation, texture, bulk density, hydraulic conductivity, depth, water storage capacity) and hydrologic processes (e.g., identification and quantification of flow paths, residence time, storage) have been monitored, characterized, and modeled at regional scales using remote-sensing techniques and at pedon scales using *in situ* instrumentation (Lin et al., 2006a). At intermediate scales (e.g., catena, field, and catchment), however, data gaps exist that need to be bridged in order to properly integrate and upscale point-based data and downscale remote sensing data (Lin et al., 2006b). Characterizing the spatial and temporal heterogeneities of the subsurface at catchment scales remains a challenging task. The resolution of most remote-sensing techniques is too coarse for site-specific use and remote sensing methods generally cannot penetrate deep into the subsurface (generally limited to top 5-6 cm of soil surface). Point-sampling methods attain various depths in the subsurface and provide accurate, high resolution data; however, such data collections are time-consuming, costly, generally destructive, and frequently confined to a limited number of sampling points. Because of these limitations, hydropedologic properties and processes for the more extensive areas among widely-spaced sampling points must be inferred. Such inferences are often based on deductions and simplified assumptions drawn from the parameters measured at the individual sampling points. The inability of point sampling methods to adequately characterize the subsurface across different soil-landscapes fosters significant ambiguity in data interpolations and model predictions (Lin et al., 2006a; Lin, 2010).

Continuous recording, noninvasive geophysical tools offer significant advantages to hydropedologic investigations at intermediate scales because of their speed, economy, ease of use, and reasonable resolution for certain subsurface features. While one-time use may provide a mapping of subsurface heterogeneity or certain features, geophysical tools are especially revealing of hydropedologic processes when these tools are used in repeated mode in different seasons over the same area or in time-lapsed manner over a certain period associated with infiltration or chemical inputs into the soil and landscape (e.g., Zhu et al., 2010a, 2010b).

Equipment:
An EM38-MK2 meter (Geonics Limited, Mississauga, Ontario) was used in this study.[1] Operating procedures for the EM38-MK2 meter are described by Geonics Limited (2007). The EM38-MK2 meter operates at a frequency of 14.5 kHz and weighs about 5.4 kg (11.9 lbs). The meter has one transmitter coil and two receiver coils, which are separated from the transmitter coil at distances of 1.0 and 0.5 m. This configuration provides two nominal exploration depths of 1.5 and 0.75 m when the meter is held in the vertical dipole orientation (VDO), and 0.75 and 0.38 m when the meter is held in the horizontal dipole orientation (HDO). In either dipole orientation, the EM38-MK2 meter provides simultaneous measurements of both apparent conductivity (EC_a) and magnetic permeability over two depth intervals.

[1] Manufacturer's names are provided for specific information; use does not constitute endorsement.

Apparent conductivity is expressed in milliSiemens/meter (mS/m). Magnetic permeability is the ratio of the secondary to primary magnetic fields and is expressed in parts per thousand (ppt).

A Trimble AG114 L-band DGPS (differential GPS) antenna (Trimble, Sunnyvale, CA) was used to georeferenced EC_a data collected with the EM38-MK2 meter.[2] An Allegro CX field computer (Juniper Systems, North Logan, UT) was used to record and store both GPS and EC_a data[2]. The RTM38MK2 program (Geomar Software, Inc., Mississauga, Ontario) was used with the EM38-MK2 meter to display and record both GPS and EC_a data on the Allegro CX field computer.[2]

To help summarize the results of the EMI survey, SURFER for Windows (version 9.0) software (Golden Software, Inc., Golden, CO) was used to construct the simulations shown in this report.[2]

The radar unit is the TerraSIRch Subsurface Interface Radar (SIR) System-3000 (here after referred to as the SIR-3000), manufactured by Geophysical Survey Systems, Inc. (GSSI; Salem, NH).[2] The SIR-3000 consists of a digital control unit (DC-3000) with keypad, SVGA video screen, and connector panel. A 10.8-volt lithium-ion rechargeable battery powers the system. The SIR-3000 weighs about 4.1 kg (9 lbs) and is backpack portable. With an antenna, the SIR-3000 requires two people to operate. Jol (2009) and Daniels (2004) discuss the use and operation of GPR. A 200 MHz antenna was used in this investigation.

The RADAN for Windows (version 6.6) software program (developed by GSSI) was used to process the radar records shown in this report.[2] Processing included: header editing, setting the initial pulse to time zero, color table and transformation selection, signal stacking, and range gain adjustments (refer to Jol (2009) and Daniels (2004) for discussions of these techniques).

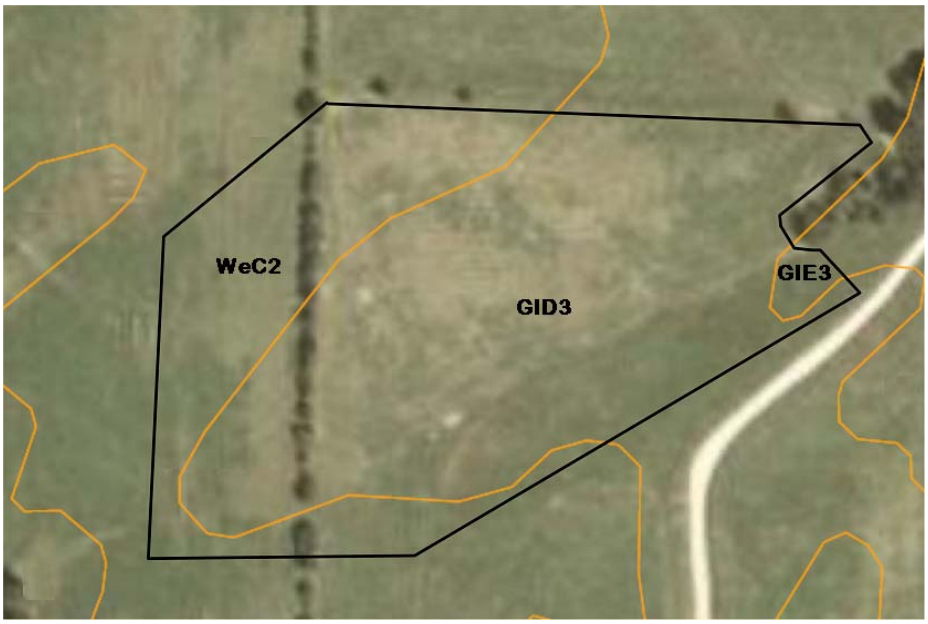

Figure 1. On this soil map from the Web Soil Survey, the boundary of the catchment is enclosed by a black-colored line.[3]

[2] Manufacturer's names are provided for specific information; use does not constitute endorsement.
[3] Soil Survey Staff, Natural Resources Conservation Service, United States Department of Agriculture. Web Soil Survey. Available online at http://websoilsurvey.nrcs.usda.gov/ accessed [5/31/2011].

Field Site:
The catchment (38.4585 N Lat., 86.7002 W Long.) is located at the Southern Indiana-Purdue Agricultural Center near Dubois, Indiana. Most of the catchment is in pasture. The extreme western portion of the catchment is under different management and is cultivated. The catchment is located in MLRA 120B - Kentucky and Indiana Sandstone and Shale Hills and Valleys, Northwestern Part. Major soil delineations within the catchment include: Gilpin silt loam, 12 to 18 % slopes, severely eroded (GID3); Gilpin silt loam, 18 to 25 % slopes, severely eroded (GIE3); and Wellston silt loam, 6 to 12 % slopes, eroded (WeC2) (see Figure 1). These well drained soils form on dissected uplands. The moderately deep Gilpin soils formed in residuum weathered from nearly horizontal interbedded shale, siltstone, and sandstone. The deep and very deep Wellston soils formed in silty loessial materials and from fine-grained sandstone or siltstone. The taxonomic classifications of these soils are listed in Table 1.

While verifying the geophysical measurements, what is assumed to be Tilsit soil was identified in three of the cores extracted within the area mapped as the Wellston consociation. These profiles were observed to contain a fine-textured 2Bt horizon that better fits the description of the Tilsit than Wellston series. The deep and very deep, moderately well drained Tilsit soils formed in silty residuum weathered from acid siltstone or fine grained sandstone. For Tilsit soils, the depth to the fragipan ranges from 46 to 71 cm. Tilsit soils have a C horizon that can be silty clay loam, sandy clay loam, or silty clay.

Table 1 - Taxonomic Classification Of The Soils Recognized At Dubois Catchment.

Soil Series	Taxonomic Classification
Gilpin	Fine-loamy, mixed, active, mesic Typic Hapludults
Wellston	Fine-silty, mixed, active, mesic Ultic Hapludalfs
Tilsit	Fine-silty, mixed, semiactive, mesic Typic Fragiudults

Field Methods:
A mobile EMI survey of the catchment was completed with the EM38-MK2 meter. The EM38-MK2 meter was mounted in a plastic sled and towed behind an ATV. The meter were operated in the deeper-sensing, vertical dipole orientation (VDO), and operated in the continuous mode with measurements recorded at a rate of 1/sec. The long axes of the meter was orientated parallel to the direction of traverse, and positioned in the sled about 2 cm above the ground surface. Apparent conductivity (EC_a) data were recorded for the shallower-sensing (0 to 75 cm), 50- and the deeper-sensing (0 to 150 cm), 100-cm intercoil spacings. All EC_a measurements were corrected to a standard temperature of 75° F.

Measurements recorded with the EM38-MK2 meter for the 50-cm intercoil spacing are suspect of errors. This intercoil spacing has been difficult to properly calibrate over electrically resistive ground and an excessive number of negative values were recorded in this catchment. As a consequence, measurements obtained with the 50-cm intercoil spacing will only be briefly mentioned in this report. The meter will be returned to Geonics Limited for recalibration and possible repairs.

Two GPR traverse lines were setup. These traverse lines span the distance between the three highest-lying monitoring stations within the catchment. These traverse lines were 57 (spanning the distance between the upper and middle enclosed monitoring stations) and 19 (partially spanning the distance from the middle to the lower station) m long. Along each line, survey flags were inserted in the ground at 3-m spacings and served as reference points. An engineering level and stadia rod was used to measure the relative elevation at each of these reference points.

Results:

EMI:

Table 2 provides basic statistics for the EC_a data that were collected with the EM38-MK2 meter. With the EM38-MK2 meter, the average EC_a increased with depth (compare measurements obtained in the deeper-sensing, 100-cm intercoil spacing with measurements obtained in the shallower-sensing, 50-cm intercoil spacing). For measurements obtained in the shallower-sensing (0 to 75 cm exploration depth), 50-cm intercoil spacing, EC_a averaged only about 6.2 mS/m, and ranged from about -63 to 107 mS/m. However, one-half of these measurements were between only about 0.9 and 8.2 mS/m.

For the deeper-sensing (0 to 150 cm exploration depth), 100-cm intercoil spacing, EC_a averaged about 27.1 mS/m and ranged from about -81 to 49 mS/m. One-half of these measurements were between about 22 and 31 mS/m. Atypically elevated positive and negative measurements are attributed to metallic artifacts scattered across the site and calibration errors.

Table 2. Apparent Conductivity Data from Site 1 – Wellsboro Soils

	EM38-MK2 50 cm	EM38-MK2 100 cm
Number	5911	5911
Minimum	-63.04	-80.98
25%-tile	0.86	22.32
75%-tile	8.17	30.63
Maximum	107.23	49.49
Average	6.25	27.09
St. Dev.	8.46	6.89

Figure 2 contains a plot of the EC_a data that were collected with 100-cm intercoil spacing. Soil boundary lines have been digitized from Web Soil Survey data.[4] The general spatial trend is for EC_a to increase towards the higher-lying summit areas in the west and northwest portions of the catchment. In general, the highest EC_a is confined to areas mapped as Wellston silt loam, 6 to 12 % slopes, eroded (WeC2). At first, this pattern was believed to principally reflect deeper depths to the underlying, electrically resistive bedrock, the thicker column of silty loessial materials, and perhaps the presence of a fragipan and perched water. However, soil cores extracted from this area suggest that the higher EC_a is principally associated with an underlying layer of fine-textured pedogenically weathered residuum. As evident in this plot, most lower-lying areas of Gilpin consociations (GID3 and GIE3), have lower EC_a. Based on limited core observations, the lower EC_a is attributed to shallower depths to bedrock, thinner sola, and the absence of a fragipan (and a perched water table) and a layer of fine-textured residuum.

[4] Soil Survey Staff, Natural Resources Conservation Service, United States Department of Agriculture. Web Soil Survey. Available online at http://websoilsurvey.nrcs.usda.gov/ accessed [5/31/2011].

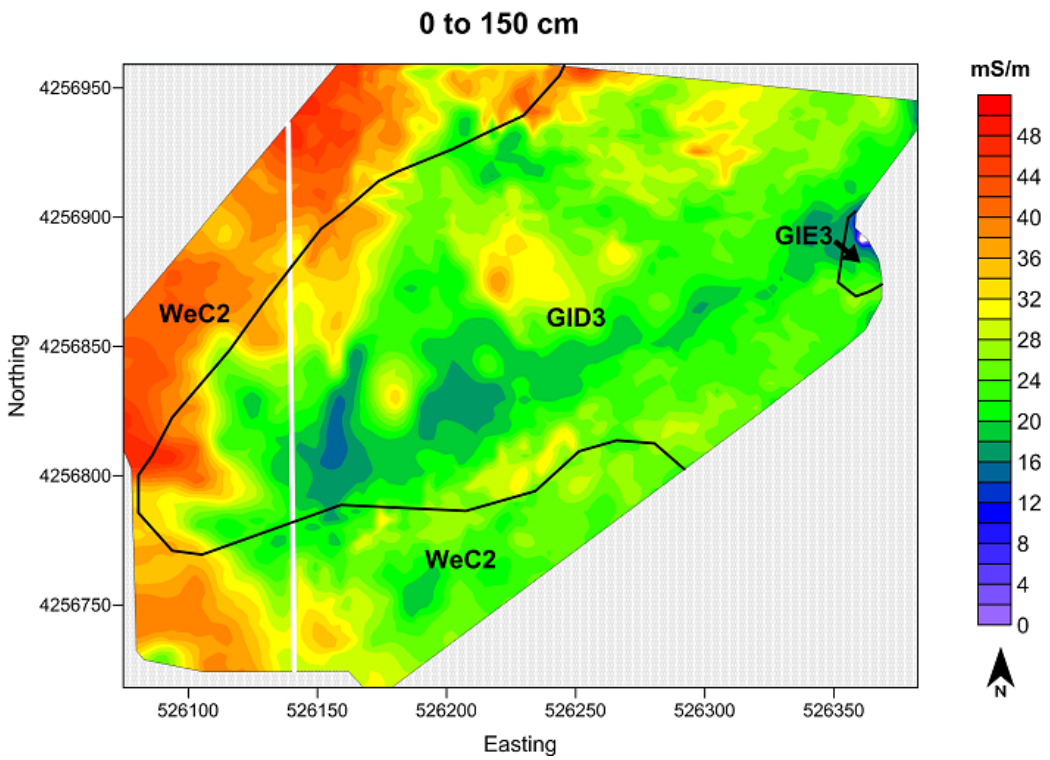

Figure 2. This two-dimensional plot of the catchment shows the spatial distribution of EC_a as measured with the EM38-MK2 meter in the VDO (nominal exploration depth of 0 to 150 cm). The white line represents a fence line separating two units of management. Soil lines have been digitized from Web Soil Survey data.

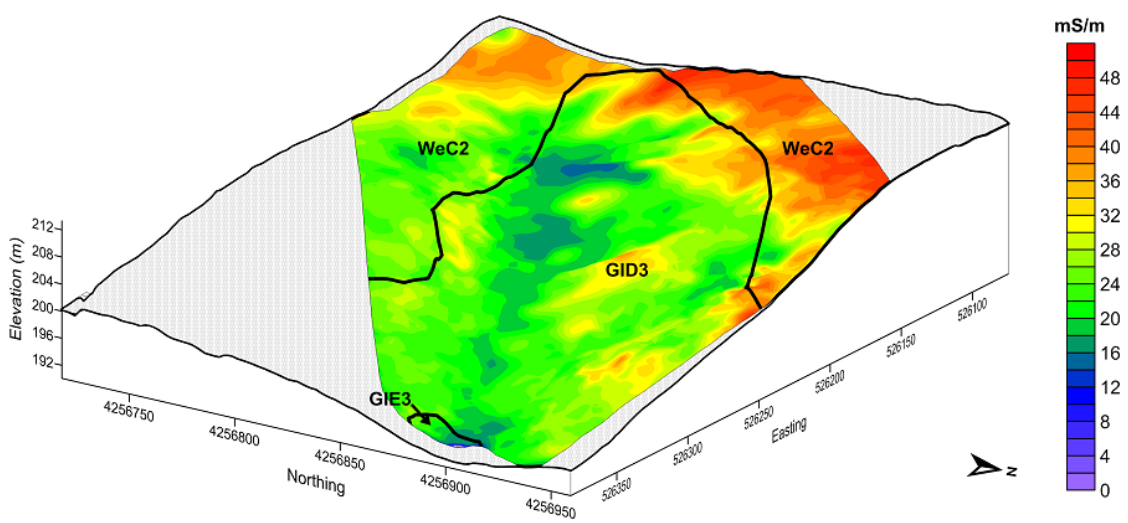

Figure 3. This three-dimensional representation of the catchment shows the spatial distribution of EC_a with reference to the soil boundary lines and landscape components.

Figure 3 contains a three-dimensional (3D) wireframe simulation of the catchment with a superimposed contour plot of the EC_a data measured with the deeper-sensing 100-cm intercoil spacing of the EM38-MK2 meter. Soil boundary lines have been digitized from Web Soil Survey data. Elevation data were derived from the AG114 GPS receiver. The association of spatial EC_a patterns with soil-landscape components is evident in this 3D simulation. Higher-lying, convex summit, shoulder, and upper side slope areas of the catchment have higher EC_a, which is principally associated with a fine-textured, water-restricting 2Bt horizon in the lower part of soil profiles. Lower-lying plane and concave side slopes and foot slopes have lower clay contents, lack the fine-textured layer, and are shallower to electrically resistive bedrock. Lower-lying toe slopes and areas that adjoin the drainageway have the lowest conductivity. While not probed, these wetter and more imperfectly drained soil-landscape components are, based on EC_a data, assumed to be composed of more electrically resistive (lower clay content) coarser-textured soil materials and/or shallower depths to bedrock. Further ground-truth core observations are needed to confirm these interpretations.

<u>GPR:</u>

Calibration of GPR:

Ground-penetrating radar is a time scaled system. The system measures the time that it takes electromagnetic energy to travel from an antenna to an interface (e.g., soil horizon, stratigraphic layer, bedrock) and back. To convert the travel time into a depth scale, either the velocity of pulse propagation or the depth to a reflector must be known. The relationships among depth (D), two-way pulse travel time (T), and velocity of propagation (v) are described in equation [1] (after Daniels, 2004):

$$v = 2D/T \qquad [1]$$

The velocity of propagation is principally affected by the relative dielectric permittivity (E_r) of the profiled material(s) according to equation [2] (after Daniels, 2004):

$$E_r = (C/v)^2 \qquad [2]$$

Where C is the velocity of propagation in a vacuum (0.298 m/ns). Typically, velocity is expressed in meters per nanosecond (ns). In soils, the amount and physical state (temperature dependent) of water have the greatest effect on the E_r and v. The dielectric permittivity ranges from 1 for air, to 78 to 88 for water (Cassidy, 2009). Small increments in soil moisture can result in substantial increases in the relative permittivity of soils (Daniels, 2004). Using a 100 MHz antenna, Daniels (2004) observed that the relative permittivity of most dry mineral soil materials is between 2 and 10, while for most wet mineral soil materials, it is between 10 and 30.

Based on the measured depth and the two-way pulse travel time to a known subsurface reflector (metal plate buried at a depth of 48 cm), the velocity of propagation and the relative dielectric permittivity through the upper part of the soil profile was estimated using equations [1] and [2]. The upper part of the soil profile was very moist at the time of this study. Water was perched above the fragipan in some cores. Through the upper part of the soil profile, the estimated E_r and v were 21.7 and 0.0644 m/ns, respectively. In areas of Tilsit-like soils, the velocity of propagation is assumed to increase and dielectric permittivity decrease in the lower part of soil profiles where soil materials were observed to be drier.

Detecting Soil Interfaces with GPR:

The amount of energy reflected back to an antenna is a function of the dielectric gradient that exists across a soil interface or boundary. The greater and/or more abrupt the contrast in the dielectric properties of adjoining soil materials, the greater the amount of energy reflected back to the antenna, and the higher the amplitude of the reflected signal appearing on radar records. Soil horizons, layers, and

features that have similar relative dielectric permittivity or gradual boundaries are poor reflectors of electromagnetic energy and are difficult to identify on radar records.

The E_r of soil materials is strongly dependent upon moisture content. As a consequence, the amount of energy reflected back to the radar's antenna is greatly influenced by the abruptness and difference in moisture contents that exist between soil horizons, layers or features. The perching of water above a relatively dense and drier fragipan (Tilsit soils) is expected to increase the difference in relative dielectric permittivity across the upper boundary of the fragipan making this interface more easily detected and traced on radar records.

Results:

Figures 4, 5, and 6 are surface normalized, sequential radar records from a 158-m long line that traversed a summit and upper side slope that were mapped as Wellston consociation in the western portion of the catchment. Surface normalization assigns elevations (measured with engineering level in field) to each user marker in the database and thereby corrects the radar record for changes in elevation. In Figures 4 to 7, the vertical scales have been compressed by a factor of 4 in order to view the entire depth profiled with GPR. Each radar record has been similarly processed.

With the relatively broad wavelength of the 200 MHz antenna, it is typically difficult to resolve features occurring within depths of 40 cm of the soil surface. On each of the displayed radar records, the upper boundary of the fragipan has been identified with a green-colored, segmented line. As evident in Figure 4 to 6, the surface pulse obscured reflections from the relatively shallow (13 to 30 cm) argillic horizon of the Tilsit-like soil, which was observed in cores, but not from the deeper (40 to 72 cm) fragipan or 2Bt horizon.

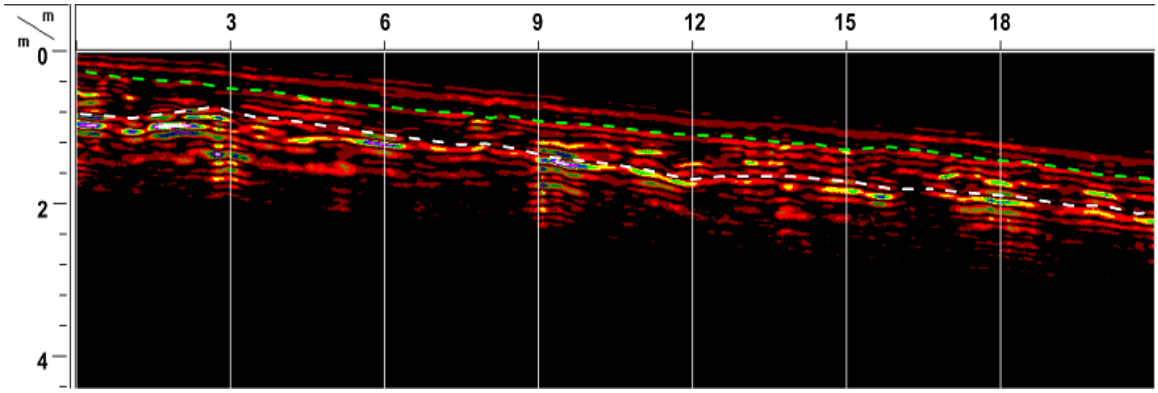

Figure 4. This radar record captures subsurface structures across the upper 21 m of a traverse spanning the distance between two monitoring well sites within the catchment. This area is mapped as Wellston silt loam, 6 to 12 % slopes, eroded (WeC2). Depth and distance scales are expressed in meters.

The deeper subsurface interface, which is highlighted by a white-colored segmented line, was identified as a 2Bt horizon that formed in fine-textured residuum. Though these GPR traverse lines crossed a portion of the catchment that was mapped as Wellston silt loam, 6 to 12 % slopes, eroded (WeC2), the observed soil cores best fit the description of Tilsit soils. The deep and very deep, moderately well drained Tilsit soils has a fragipan at depth ranging from 46 to 71 cm and has a C horizon that can be silty clay loam, sandy clay loam, or silty clay.

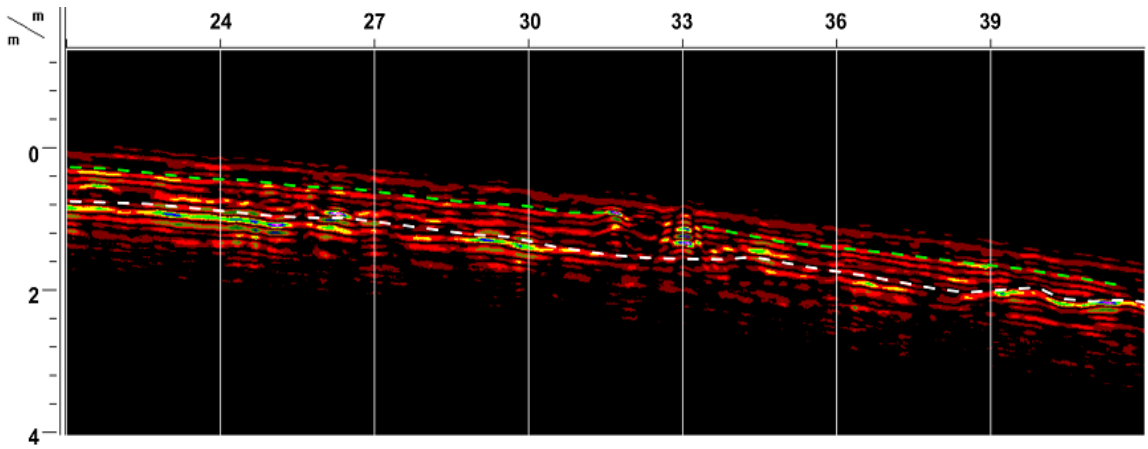

Figure 5. This radar record captures subsurface structures across the 21 to 42 m section of a traverse spanning the distance between two monitoring well sites within the catchment. This area is mapped as Wellston silt loam, 6 to 12 % slopes, eroded (WeC2). Depth and distance scales are expressed in meters.

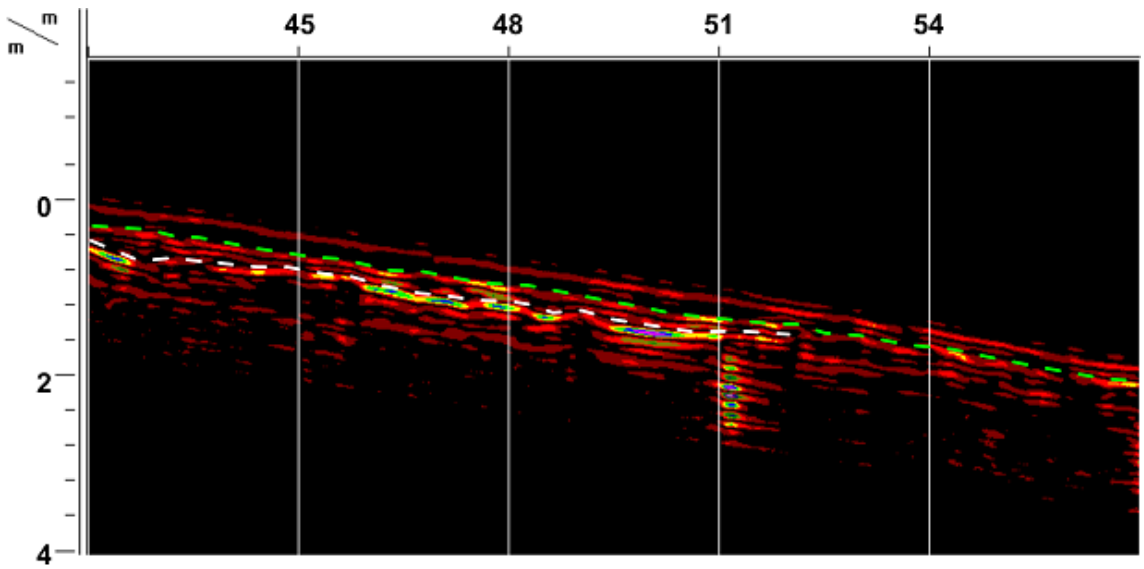

Figure 6. This radar record captures subsurface structures across the lower 42 to 57 m of a traverse spanning the distance between two monitoring well sites within the catchment. Depth and distance scales are expressed in meters.

Multiple reflections from both the fragipan and the 2Bt horizon are evident on the radar records shown in Figure 4, 5, and 6. These layers appear laterally continuous, but vary in amplitude suggesting spatially varying soil properties across these interfaces (leading to differences in the amplitude of the reflected signals). For the first 33-m of this traverse line (see Figures 4 and 5), these interfaces closely parallel the soil surface. The interface marking the contact of the loessial deposits with the underlying fine-textured residuum is more strongly expressed (higher amplitude signals shown in shades of white, blue, green, and yellow with the selected color table) than the fragipan. The higher amplitude is associated with an abrupt change in clay and related moisture contents at this interface (upper boundary of 2Bt horizon). However, from distance of about 33- to 52-m along this traverse line, the upper boundary of this interface (2Bt

horizon) becomes wavier and less deep, a change that should impact hydrologic processes. A knickpoint in the radar imagery is evident between about the 32 to 33 meters distance marks (see Figure 5). The source of this interruption in the radar imagery was not investigated, but the reflection patterns suggest a filled excavation and/or large point object(s) (e.g., large rock fragment). The 2Bt horizon appears to end near the 52-m mark (see Figure 6). The fragipan and the 2Bt horizon represent layers that will influence the flow of water and hydrologic processes. In Figure 2 and 3, the distribution of higher EC_a (>30 mS/m) is believed to correspond to the distribution of clayey residuum and Tilsit-like soils, and the upper 52 m of this radar traverse line.

Figure 7 is a surface-normalized radar record that was collected on a lower side slope component within the catchment. The area traversed with GPR is mapped as Gilpin silt loam, 12 to 18 % slopes, severely eroded (GID3). Two cores extracted from this area, but were depth restricted because of auger refusal on either a large rock fragment or bedrock. In Figure 7, a segmented, white-colored line has been used to indicate the interpreted depth to bedrock. Compared with the radar records that were collected on higher-lying slope components (Figures 4, 5, and 6), other than the soil/bedrock interface and bedding planes within the bedrock, the radar record shown in Figure 7 lacks reflection from soil horizons.

The bedrock underlying the Gilpin consociation is described as consisting of interbedded layers of shale, siltstone, and sandstone. Differences in lithology are suggested on the radar record shown in Figure 7. In the extreme left-hand portion of the radar record (near "A" in Figure 7) high amplitude, planar reflectors suggest highly contrasting sedimentary beds. Along this traverse line, beds become more weakly expressed (shades of red and black with the selected color table) from about the 5- to 19-m distance marks. Soils on lower slope components appear to be underlain by a softer, less contrasting lithology than the bedrock components that underlie the initial 5-m of this traverse line. Based on soil depth classes, soils are interpreted to be 18 % shallow, 65 % moderately deep, and 17 % deep on the radar record shown in Figure 7.

Within the catchment, GPR can be used to identify soils based on soil depth criteria, profile the bedrock topography, and characterize soil, lithologic and stratigraphic layers. However, in some areas of shallow to deep soils, because of lack of sufficient contrast in physical properties (water content, composition, fabric, grain size, and structure, and density) between the soil and underlying bedrock, the soil/bedrock interface is more poorly defined and interpretation more uncertain.

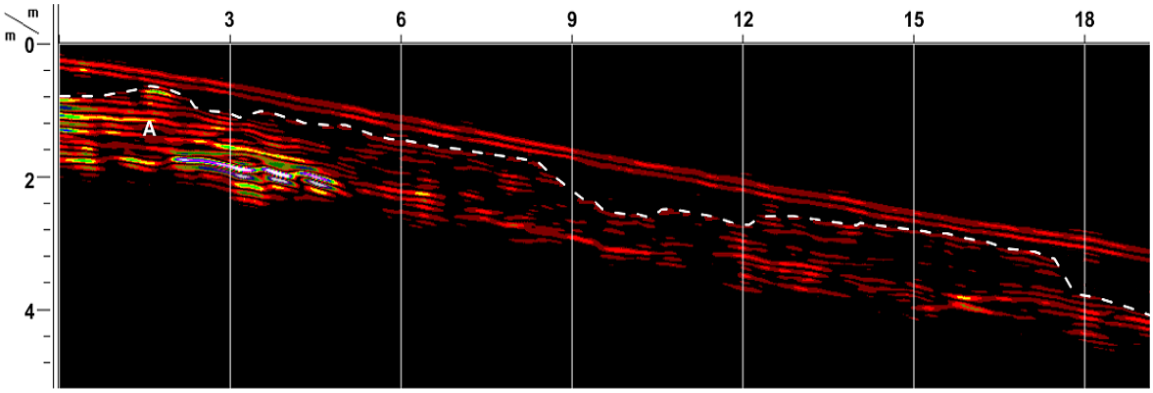

Figure 7. This radar record is from a lower side slope of the catchment that is mapped as Gilpin silt loam, 12 to 18 % slopes, severely eroded (GID3). The segmented white-colored line indicates the interpreted depth to interbedded shale, siltstone, and some sandstone bedrock.

Other than the soil/bedrock interface and strata within the bedrock units, no soil interface is evident on the radar record shown in Figure 7. While Gilpin soils have an argillic horizon, it is too shallow (15 to 25 cm) to be resolved with the 200 MHz antenna. In contrast with the radar records collected over the area of Tilsit-like soils (Figures 4 to 6), the radar record collected over the area of Gilpin soils (Figure 7), other than the soil/bedrock interface, lacks moderate and high amplitude reflections in the soil profile which would suggests the presence of well expressed and water restricting layers.

Compared with the area of Tilsit soils, the lower clay content and the presence of electrically resistive bedrock at shallower depths are factors believed to be responsible for the lower EC_a (20 to 28 mS/m) in areas of Gilpin soils (see Figure 2 and 3) and along the radar traverse shown in Figure 7.

References:

Bui, E.N., 2004. Soil survey as a knowledge system. *Geoderma* 120: 17-26.

Cassidy, N.J. 2009. Electrical and magnetic properties of rocks, soils, and fluids. In *Ground Penetrating Radar: Theory and Applications*, ed. H. M. Jol, 41-72 pp. Elsevier Science, Amsterdam, The Netherlands.

Daniels, D.J., 2004. *Ground Penetrating Radar; 2nd Edition*. The Institute of Electrical Engineers, London, United Kingdom.

Geonics Limited, 2007. EM38-MK2 ground conductivity meter operating manual. Geonics Ltd., Mississauga, Ontario.

Jol, H., 2009. Ground Penetrating Radar: Theory and Applications. Elsevier Science, Amsterdam, The Netherlands.

Lin, H., 2010. Earth's Critical Zone and hydropedology: concepts, characteristics, and advances. *Hydrology and Earth System Sciences* 14: 25-45.

Lin, H.S., J. Bouma, Y. Pachepsky, A. Western, J. Thompson, M. Th. van Genuchten, H. Vogel, and A. Lilly, 2006a. Hydropedology: Synergistic integration of pedology and hydrology. *Water Resource Research* 42, W05301, doi: 10.1029/2005WR004085.

Lin, H.S., W. Kogelmann, C. Walker, and M.A. Burns, 2006b, Soil moisture patterns in a forested catchment: A hydropedological perspective. *Geoderma* 131: 345-368.

Zhu, Q., H.S. Lin, and J.A. Doolittle. 2010. Repeated electromagnetic induction surveys for determining subsurface hydrologic dynamics in an agricultural landscape. *Soil Science Society of America, J.* 74: 1750-1762.

Zhu, Q., H.S. Lin, and J.A. Doolittle. 2010. Repeated electromagnetic induction surveys for improved soil mapping in an agricultural landscape. *Soil Science Society of America, J.* 74: 1763-1774